PROCESSING AND PROPERTIES OF SELF-ALIGNED GRAPHENE/EPOXY NANOCOMPOSITES

Nariman Yousefi, Qingbin Zheng, XiuYi Lin, Kan Kan Yeung, Jang-Kyo Kim*

*Department of Mechanical Engineering, The Hong Kong University of Science and Technology, Clear Water Bay, Kowloon, Hong Kong *mejkkim@ust.hk*

Keywords: Nanocomposites, Self-alignment, Epoxy, Graphene

Abstract

The mechanical, thermal and electrical properties of epoxy/graphene oxide (GO) composites are studied. GO aqueous dispersion is introduced to waterborne epoxy latex and the GO sheets are chemically reduced before curing to produce composites. The epoxy latex particles not only form a continuous matrix but also stabilize the hydrophobic reduced GO (rGO). The chemical reduction improves the mechanical and thermal properties of the nanocomposites by facilitating the interaction between polymer molecules and graphene sheets. The monolayer graphene sheets with a high aspect ratio self-align into a layered structure above a critical concentration thanks to the low viscosity of aqueous dispersion and a long processing time. The aligned graphene nanocomposites display significant anisotropy where the steady-state electrical conductivity along the in-plane direction is three orders of magnitude higher than that of the perpendicular direction. The origins and the practical implications of the self-aligned layered structure of nanocomposites are discussed.

1 Introduction

Being one of the strongest materials, graphene has attracted tremendous attention recently as a nanoscale reinforcement of a wide range of polymer composites [1,2]. Graphene and graphene oxide (GO) have been extensively used in different matrices to improve the mechanical, electrical, thermal, magnetic and gas permeation properties, to name a few [3-5]. Among many different methods for the production of graphene, such as mechanical cleavage, chemical vapor deposition (CVD) and epitaxial growth, the chemically derived GO from natural graphite through thermal exfoliation of graphite intercalated compounds (GIC) and subsequent oxidization and exfoliation of GICs is proven to be the most efficient for many nanocomposite applications owing to the scalability and relative simplicity of the processing method. The resultant GO contains a wide array of functional groups which upon dissociation in water form a stable colloidal dispersion [6,7]. However, a chemical or thermal reduction step is often needed to restore the sp^2 conjugated structure and electrical conductivity of the insulating GO. This often happens at the expense of dramatic reduction in hydrophilicity and stability of the GO sheets [8,9]. Therefore, obtaining a well-dispersed and engineered nanostructure is a challenge in most polymeric systems. On the other hand, some functional applications require ordered arrangements, such as layered structures of nanofillers in a matrix to ensure certain properties along the alignment direction. Although bottom up approaches, such as Langmuir-Blodgett assembly, address this need to a certain extent [10], these techniques are extremely time consuming to prepare layered nanocomposites on a large scale for real life applications.

Waterborne polymers are gaining increasing interests as their processing method is aqueous, benign and environmentally friendly [11]. Furthermore, GO is highly stable and can be well-dispersed in an aqueous medium. Therefore, waterborne polymers can be a good option for the preparation of well-dispersed graphene nanocomposites. Further to our recent progress in synthesizing ultra-large GO and observation of liquid crystallinity in aqueous GO dispersions [10,12], we prepared waterborne epoxy nanocomposites containing well-dispersed rGO sheets. The reduction of graphene oxide played a major role in improving the electrical, thermal and mechanical properties of the nanocomposites. The low viscose aqueous medium and large aspect ratio of the GO sheets resulted in self-alignment into a layered structure.

2 Materials and Testing Methods

Aqueous dispersion of GO was produced using a modified Hummers method from expanded graphite (Asbury Mills). The detailed procedure for the preparation of ultra-large GO is explained in our previous publications [10,12]. The GO dispersion was mixed with aqueous emulsions of epoxy resin (Kukdo Chemicals) and stirred for 1 h. Hydrazine solution at a ratio of 3:1 was then added and the mixture was stirred at 80°C for 24 h. The mixture was then cooled down to room temperature and a required amount of water emulsifiable hardener was added. The mixture was poured into a flat, rectangular mold and cured in an oven at 60°C for 24 h to obtain homogenous composite films (Fig. 1).

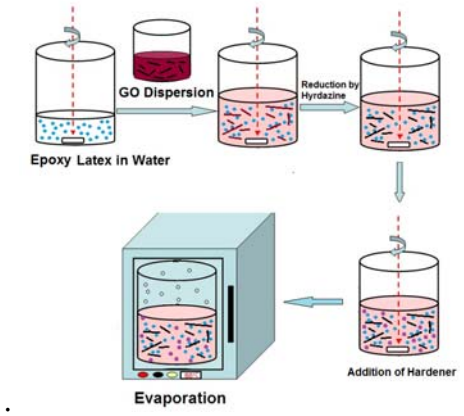

Figure 1. Schematic illustration of composite fabrication.

The stability of composite dispersions with different graphene concentrations was measured using a Zeta potential analyzer (Brookhaven ZetaPlus) at room temperature. The GO and epoxy/rGO composites were examined under a transmission electron microscope (TEM, JEOL 100X). The samples were prepared from the droplets of the dispersions on a carbon grid. The fracture surface of the composite films was examined on a scanning electron microscope (SEM, JEOL 6390F).

Raman spectroscopy (Reinshaw MicroRaman/Photoluminiscence System) was used to study the anisotropic nature of the nanocomposite films. The composite samples were mounted in an epoxy resin holder in the vertical and horizontal orientations to obtain the polarized spectra. He-Ne laser with a wave-length of 632.8 nm was used in all experiments. The electrical conductivities of the nanocomposite films were measured in both the in-plane and through-the-thickness directions at ambient temperature. The conductivities along the in-plane direction were measured based on the four-point probe method using a resistivity/Hall

measurement system (Scientific Equipment & Services). The through-the-thickness conductivities were measured using a Sony Tektronix A370 curve tracer. To reduce the contact resistance between the probes and the film surface, the samples were coated with silver paste at contact points. The tensile tests were conducted on a dynamic mechanical analyzer (DMA 7, Perkin Elmer). The composite films were cut into 15 long ×3mm wide rectangular strips. All tensile tests were conducted in a controlled force mode with a preload of 100 mN and a force ramp rate of 100 mN/min. The T_g was measured on a differential scanning calorimeter (DSC, QA 1000, TA Instruments) and the thermal degradation behavior was studied on a thermogravimetric analyzer (TGA, Q 5000, TA Instruments) both at a ramp rate of 10°C/min in a nitrogen atmosphere.

3 Results and Discussions

3.1 Stability of Epoxy/rGO Dispersion

GO sheets readily dispersed in water due to the presence of the oxygenated functional groups on their basal plane and edges. Recent studies show that the edge functional groups in GO ionize in water and introduce a negative charge on the GO sheets [13-16]. The repulsive force experienced by neighboring GO sheets is the key underlying mechanism for colloidal stability of the GO/water system. However, GO is insulating and to revert conductivity one needs to reduce GO to restore the conjugated sp^2 structure. Upon reduction, most of the oxygenated functional groups on the surface of GO were eliminated, hence the stability of rGO was disrupted, resulting in severe agglomeration of rGO in most organic solvents. However, when reduced in presence of epoxy, a stable dispersion was formed which could be retained for months.

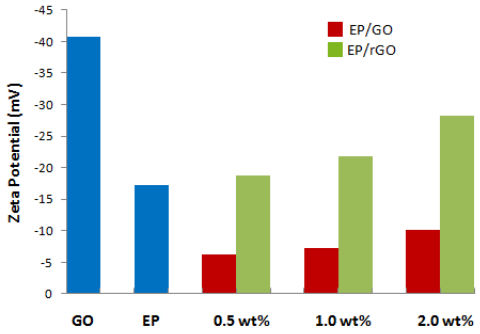

Figure 2. Zeta potential of GO, epoxy, epoxy/1wt% GO and epoxy/1wt% rGO.

The Zeta potentials shown in Fig. 2 indicates that both GO and epoxy were negatively charged, and upon mixture to form a composite the absolute Zeta potential decreased (in the negative direction). However, upon reduction the absolute Zeta potential value increased about three times beyond that of the epoxy/GO mixture, suggesting the formation of a highly stable dispersion. It is postulated that the epoxy particles form a uniform, continuous layer on the surface of rGO sheets, making them stable within it. The TEM images of GO and epoxy/rGO (Figs. 3a and 3c, respectively) suggest the formation of a layer on rGO surface, as indicated by the material with darker color. It appears that the epoxy latex particles adhered to the rGO surface and fused together to form a continuous layer with a negative charge, see the schematic in Fig. 3d. A similar mechanism for the formation of a uniform polymeric layer on rGO sheets has been reported for other nanocomposites containing, e.g. polystyrene and polyurethane [11,17]. Apart from guaranteeing a highly stable colloid, this phenomenon can ensure molecular level dispersion of rGO in the epoxy matrix.

3.2 self-alignment of rGO and mechanical properties

Considering the large aspect ratio of rGO nanosheets and the low viscose processing medium, a high degree of self-alignment in epoxy/rGO nanocomposites is expected. SEM micrographs of the fracture surface of epoxy/rGO at different contents show a transition from random distribution at 0.5wt% to an oriented structure at 2wt% (Fig. 4).

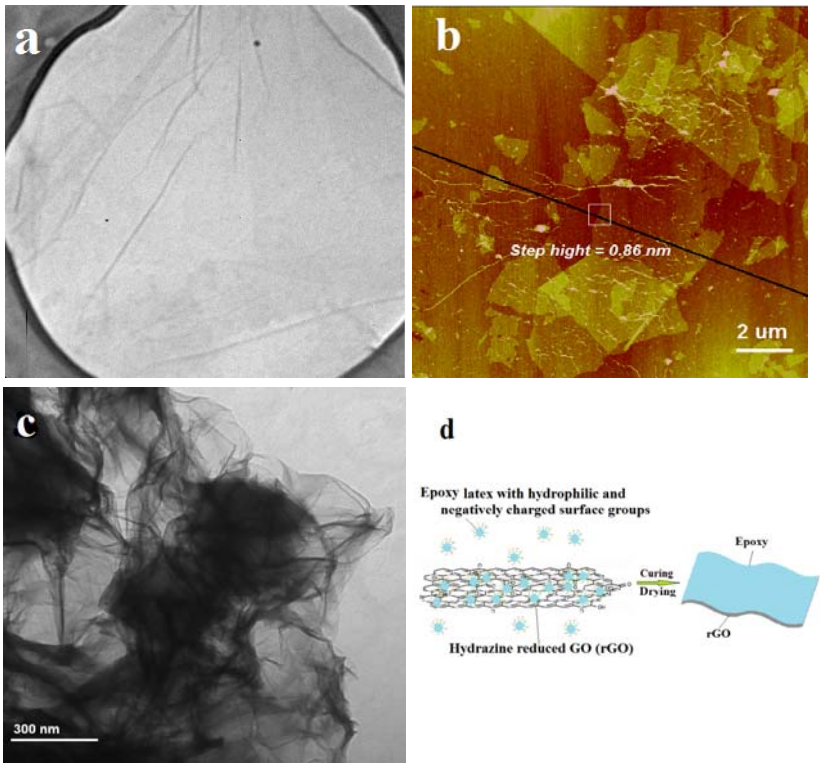

Figure 3. (a) TEM and (b) AFM images of a monolayer GO, (c) TEM image of epoxy covered rGO sheets; and (d) a schematic of stabilization through formation of an epoxy layer on rGO surface.

Random dispersion of nanosheets at low rGO content is thermodynamically favorable as the total entropy of the system is maximized. However, at higher rGO contents, the excluded volume between graphene sheets dictates a self-aligned structure. In other words, when water evaporated, the graphene sheets tended to align their basal planes so that a layered structure was formed after complete evaporation of water. The high aspect ratio of the graphene nanosheets and low viscosity of dispersion medium had a large influence on the formation of the self-aligned nanostructure. This finding is in line with the recent observation of liquid crystallinity in aqueous GO dispersions [6, 12].

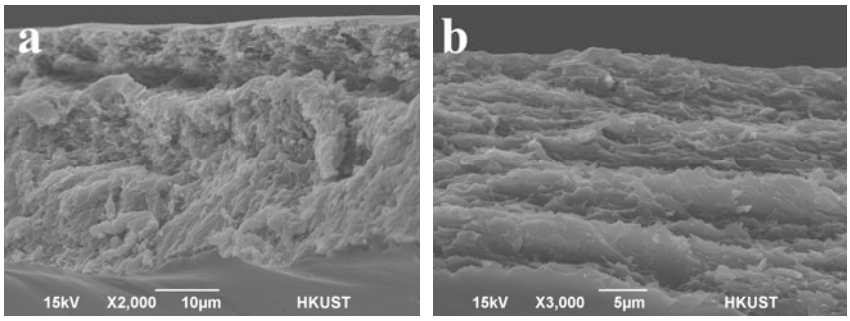

Figure 4. Typical SEM images of fracture surface of (a) 0.5 wt% and (b) 2 wt% epoxy/rGO nanocomposites.

Alignment of graphene sheets in high concentration samples can further be verified by polarized Raman spectroscopy. A remarkable difference in the Raman peaks of aligned CNTs in different matrices has been reported [18-20]. The Raman spectra corresponding to the composites with a low graphene concentration were almost identical in both the in-plane and perpendicular directions (Fig. 5), whereas those corresponding to the high graphene concentration displayed a remarkable difference between the two directions. The Raman resonance was more prominent when the incident beam was parallel to the alignment direction than transverse to it.

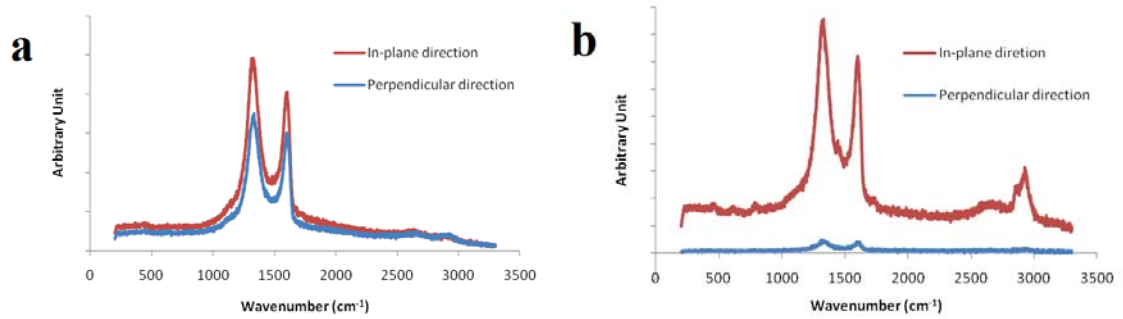

Figure 5. Polarized Raman spectra of (a) 0.5 wt% and (b) 2 wt% epoxy/rGO nanocomposites along the in-plane and perpendicular directions.

The alignment of graphene at its high concentration brought about interesting properties to the nanocomposites. There was significant anisotropy or an indication of anisotropy between the properties measured for composites with low and high graphene contents as well as those measured along the in-plane and perpendicular directions of alignment. The up-surge in Young's modulus and tensile strength (Fig. 6a) at around 1wt% is probably a result of the transition from the random to aligned GO sheets.

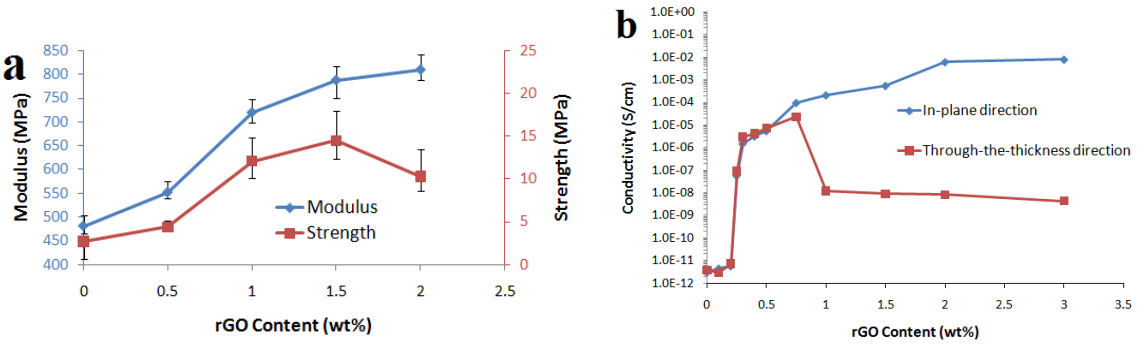

Figure 6. (a) Young's modulus and tensile strength; and (b) electrical conductivity of epoxy/rGO nanocomposites along the in-plane and perpendicular directions as a function of rGO content.

3.3 Thermal Properties

Interactions between polymer molecules and nanofillers have a prominent effect on the thermal properties, such as glass transition temperature (T_g) and degradation behavior of the nanocomposites. The T_g and the temperatures corresponding to onset of thermal degradation and 50% weight loss of the nanocomposites are presented in Table 1. The T_g consistently increased with increasing graphene content, the increment being more prominent for the composites containing rGO than those with GO. This observation is clear evidence of higher molecular interactions between the polymer molecules and graphene sheets upon chemical

reduction. Although the reduction of GO had no visible difference in the onset of degradation temperature, it significantly affected the temperature for 50% weight loss.

Sample	T_g (°C)	Degradation onset (°C)	50% weight loss temperature (°C)
Neat Epoxy	62.0	371	402
Epoxy/0.5 GO	63.0	369	409
Epoxy/1.0 GO	65.1	366	410
Epoxy/1.5 GO	66.3	367	414
Epoxy/2.0 GO	68.0	368	416
Epoxy/1.0 rGO	70.2	369	418
Epoxy/1.5 rGO	80.0	370	419

Table 1. Thermal properties of epoxy/GO and epoxy/rGO nanocomposites.

3.4 Electrical Conductivity

Conducting polymer nanocomposites find many applications, such as electromagnetic shielding, conductive coatings and films, sensors, etc. A percolation behavior is seen when the composite rapidly becomes conductive as the conductive filler content exceeds a critical threshold in an insulating matrix [21,22]. Formation of networks of conductive fillers is the main reason behind this transition. The electrical conductivity of the epoxy/rGO composites is measured in two directions at different rGO contents (Fig. 6b). A percolation threshold as low as 0.26 wt% was obtained in the in-plane direction, due to the high aspect ratio of the graphene sheets. The comparison of the conductivities measured along the perpendicular direction with in-plane direction revealed a high degree of anisotropy of the nanocomposites containing high rGO contents: the conductivity either increased or decreased beyond the rGO content at about 0.75wt% depending on the measurement direction. The significant anisotropy is a reflection of the preferential alignment of rGO sheets. The alignment of rGO sheets means that there were more conducting networks along the in-plane direction than perpendicular to it.

4 Conclusions

Epoxy/rGO nanocomposites were produced based on the solution casting method, which presented significant improvements in mechanical, thermal and electrical properties compared to the neat epoxy. It is proposed that a uniform epoxy layer was formed on rGO surface, making the epoxy/rGO dispersion highly stable. When graphene content exceeded a critical value, the rGO sheets tended to self-align to form a layered structure with significant anisotropy in the properties of the nanocomposites. The alignment had an ameliorating effect on in-plane mechanical and electrical properties, at the expense of less significant improvements of the properties in the through-thickness direction. Reduction of GO also had a positive effect on the interaction between the polymer molecules and graphene sheets with an associated increase in T_g of the nanocomposites.

Acknowledgements

The project was supported by the Research Grants Council of Hong Kong SAR (Project Number: 614010, 613811). NY was a recipient of the Hong Kong PhD Fellowship.

References

[1] Stankovich S., Dikin D.A., Dommett G.H.B., Kohlhaas K.M., Zimney E.J., Stach E.A., Piner R.D., Nguyen S.T., Ruoff R.S. Graphene-based composite materials. *Nature*, **442**, pp. 282-286 (2006).

[2] Potts J.R., Dreyer D.R., Bielawski C.W., Ruoff R.S. Graphene-based polymer nanocomposites. *Polymer*, **52**, pp. 5-25 (2011).
[3] Ramanathan T., Abdala A.A., Stankovich S., Dikin D.A., Herrera A.M., Piner R.D., Adamson D.H., Schniepp H.C., Chen X., Ruoff R.S., Nguyen S.T., Aksay I.A., Pru d'Homme R.K., Brinson L.C. Functionalized graphene sheets for polymer nanocomposites. *Nat. Nanotechnol.*, **36**, pp. 327-331 (2008).
[4] Kim H.W., Abdala A.A., Macosko C.W. Graphene/polymer nanocomposites *Macromolecules*, **43**, pp. 6515-6530 (2010).
[5] Cai D. Y., Song M. Recent advance in functionalized raphene/polymer anocomposites *J. Mater. Chem*, **20**, pp. 7906-7915 (2010).
[6] Guo F., Kim F., Han T.H., Shenoy V.B., Huang J.X., Hurt R.H. Hydration-Responsive Folding and Unfolding in Graphene Oxide Liquid Crystal Phases, *ACS Nano*, **5**, pp. 8019-8025 (2011).
[7] Geng Y, Wang S.J., Kim J.K. Preparation of graphite nanoplatelets and graphene sheets. *J Colloid Interf. Sci.* **336**, pp. 592–598 (2009).
[8] Tkalya E., Ghislandi M., Alekseev A., Koning C., Loos J.. Latex-based concept for the preparation of graphene-based polymer nanocomposites. *J. Mater. Chem.*, **20**, pp. 3035-3039 (2010).
[9] Li D., Muller M.B., Gilje S., Kaner R.B., Wallace G.G. Processable aqueous dispersions of graphene nanosheets. *Nat. Nanotechnol.*, **3**, pp. 101-105 (2008).
[10] Zheng Q.B., Ip W.H., Lin X.Y., Yousefi N., Yeung K.K., Li Z., Kim J.K. Transparent Conductive Films Consisting of Ultra-Large Graphene Sheets Produced by Langmuir-Blodgett Assembly. *ACS Nano*, **5**, pp. 6039-6051 (2011).
[11] Yousefi N, Gudarzi M.M., Zheng Q.B., Aboutalebi S.H., Sharif F. Kim J.K. Self-alignment and high electrical conductivity of ultralarge graphene oxide/polyurethane nanocomposites. *J. Mater. Chem.*, DOI:10.1039/C2JM30590A (2012).
[12] Aboutalebi S.H., Gudarzi M.M. , Zheng Q.B., Kim J.K. Spontaneous Formation of Liquid Crystals in Ultralarge Graphene Oxide Dispersions. *Adv. Funct. Mater.*, **21**, pp. 2978-2988 (2011).
[13] Cote L.J., Kim J.Y., Tung V.C., Luo J.Y., Kim F., Huang J.X. Graphene oxide as surfactant sheets. *Pure Appl. Chem.*, **83**, pp. 95-110 (2011).
[14] Li Y.G., Wu Y.Y. Coassembly of Graphene Oxide and Nanowires for Large-Area Nanowire Alignment. *J. Am. Chem. Soc.* **131**, pp. 5851-5857 (2009).
[15] Gao W., Alemany L.B., Ajayan P.M. New insights into the structure and reduction of graphite oxide. *Nat. Chem.* **1**, pp. 403-408 (2009).
[16] Liang J.J., Xu Y.F., Huang Y., Zhang L., Wang Y., Ma Y.F., Li F.F., Guo T.Y., Chen Y. Infrared-Triggered Actuators from Graphene-Based Nanocomposites. *J. Phys. Chem. C* **113**, pp. 9921-9927 (2009).
[17] Fang M., Wang K.G., Lu H.B., Yang Y.L., Nutt S. Single-layer graphene nanosheets with controlled grafting of polymer chains. *J. Mater. Chem.*, **19**, pp. 7098-7105 (2009).
[18] Wang Q., Dai J.F., Li W.X., Wei Z.Q., Jiang J.L. The effects of CNT alignment on electrical conductivity and mechanical properties of SWNT/epoxy nanocomposites. *Compos. Sci. Technol.*, **68**, pp. 1644-48 (2008).
[19] Chen W., Tao X.M. Production and characterization of polymer nanocomposite with aligned single wall carbon nanotubes. *Appl. Sur. Sci.*, **252**, pp. 3547-3552 (2006).
[20] Haggenmueller R., Gommans H.H., Rinzler A.G., Fischer J.E., Winey K.I. Aligned single-wall carbon nanotubes in composites by melt processing methods. *Chem. Phys. Lett.*, **330**, pp. 219-225 (2000).
[21] Li J., Kim J.K. Percolation threshold of conducting polymer composites containing 3D randomly distributed graphite nanoplatelets. *Compos. Sci. Technol.*, **67**, pp. 2114-2120 (2007).

[22] Li J., Ma P.C., Sze C.W., Kai T.C., Tang B.Z. and Kim J.K. Correlations between percolation threshold, dispersion state and aspect ratio of carbon nanotube. *Adv. Funct. Mater.* **17**, pp. 3207-3215 (2007).